Supplementary Information (SI) for Journal of Materials Chemistry A.
This journal is © The Royal Society of Chemistry 2026

Densification-driven power factor enhancement in Cu-MOF hybridization carbon nanotube composites for waste heat recovery across broad temperature ranges

Qiong Guo[1,2,3], Zihan Zhu[1,2,3], Hong Wang[1,2,3]*

[1] Frontier Institute of Science and Technology, Xi'an Jiaotong University, Xi'an, 712046, China

[2] State Key Laboratory of Multiphase Flow in Power Engineering, Xi'an Jiaotong University, Xi'an, 710049, China

[3] School of Energy and Power Engineering, Xi'an Jiaotong University, Xi'an, 710049, China

E-mail: hong.wang@xjtu.edu.cn

Materials and methods

Materials

Single-walled carbon nanotube S22 (CNT, diameter range: 1~2 nm) was purchased from Nanjing XFNANO Materials Tech. Co. Ltd, China. 4-hydroxythiophenol was purchased from Energy Chemical Co., Ltd., China. Copper(I) oxide was provided by Beijing Ouhe Technology Co., Ltd., China. Polyethyleneimine (PEI) (99 %) was purchased from Macklin Co., Ltd., China. Ethanol was purchased from Tianjin Fuyu Fine Chemical Co., Ltd., China. Silver conductive paint was purchased from Electron Microscopy Sciences Co., Ltd., China. All the commercially available reagents and solvents were used as received without further purification except otherwise specified.

Characterization

Compress the composites strips was used by tablet press (YLJ 24T, HEFEI KEJING). The morphology and elemental distribution of a substance were tested by scanning electron microscope (SEM, ZEISS Gemini SEM 500) and Oxford EDS System (Ultim Max100). The chemical structures were analyzed by Fourier Transfor Infrared spectrometer (FT-IR, Bruker VERTEX70, Germany) in 4000–400 cm^{-1}. The crystal features were identified by XRD (Bruker D8 ADVANCE, China) using Cu Kα (λ = 1.54 Å) radiation source (40.0 kV, 40.0 mA). The bandgap was confirmed by analyze the absorption peak obtained from UV-Vis-NIR (PE Lambda950). Thermogravimetric (TG, SDT Q600, TA) was employed to investigate the thermostability which were performed under a nitrogen atmosphere with a heating rate of 10 ℃·min^{-1}. The electrical conductivity and Seebeck coefficient were measured by the JouleYacht MRS-3RT thin film thermoelectric test system. The thermal conductivity was measured by LFA-467, NETZSCH, Germany. The electrical conductivity at low temperature was measured by JouleYacht MRS-3 thin film thermoelectric test system. The electrical conductivity and Seebeck coefficient of samples at high temperature were measured by using a commercial equipment (NETZSCH, SBA-458, Germany). The output voltage and output

power of the thermoelectric device were measured by Keithley 2400. Pen-type ultrasonic (FS-250N, 105W) and bath-type ultrasonic (Bransonic M2800H-C, 110W) were used to sonicate the mixture solution. The tablet press (YLJ-24T, HEFEI KEJING) provided the pressure to the film. All properties were averaged to get the real properties. The error (E) is calculated according to the following equation:

$$E = \sqrt{\sum_{i=1}^{n} (X_i - X_m)^2 / n}$$

The value of corresponding property experimental data (X_m) is calculated as follows:

$$X_m = \sum_{i=1}^{n} X_i / n$$

The Synthesis of 1D CP-SL

CP-SL were synthesized by a modified approach in the previous work. [1-3] 4-hydroxythiophenol (1.10 g, 8.72 mmol) was added into absolute ethanol (100 mL) suspension of freshly prepared copper(I) oxide (0.50 g, 3.50 mmol) in a glass bottle. The mixture was purged by argon for 10 min to remove oxygen and then refluxed at 85℃ for 20 min. The resultant product was filtered, washed with ethanol for three times, and then dried under vacuum at 60℃ for 6 h to furnish a reddish brown solid (0.76 g). The as-synthesized sample was labeled as 1D CP-SL.

The Synthesis of p-type 1D CP-SL/CNT composites strips

Single carbon nanotubes were dispersed in 50 mL of the absolute ethanol solution. Subsequently, the mixed solution was sonicated with a pen-type ultrasonic for 2 h and then a bath-type ultrasonic for another 2 h. 4-hydroxythiophenol and copper(I) oxide were added to the above mixture solution and stirred at 85℃ for 20 min with the protection of argon. Then the composites can be obtained by vacuum filtration, washed with ethanol, and

dried under vacuum at 60℃ for 6 h. We investigate the composite films under different concentrations, while controlling other variables unchanged. As-prepared p-type composite films are denoted as 1D CP-SL/CNT_x, where x indicates the CNT weight fraction (wt.%).

Type	CNT (g)	4-hydroxythiophenol (g)	copper(I) oxide (g)
1D CP-SL/CNT_{50}	0.010	0.050	0.001
1D CP-SL/CNT_{40}	0.010	0.070	0.015
1D CP-SL/CNT_{20}	0.010	0.150	0.035
1D CP-SL/CNT_{10}	0.005	0.100	0.035
1D CP-SL/CNT_{2}	0.005	0.500	0.180

The Synthesis of n-type 1D CP-SL/PEI-CNT composites strips

Single carbon nanotubes were dispersed in 20 mL of the absolute ethanol solution. The mixed solution was sonicated with a pen-type ultrasonic for 2 h, added n-type dopant PEI into the CNT solution, then took a bath-type ultrasonic for another 2 h. Subsequently, 1D CP-SL was added into and the absolute ethanol solution (10 mL), stirred vigorously for 12 h by using a magnetic stirrer, added to PEI/CNT solution, stirred vigorously for 5 min at 25℃, vacuum filtrated, washed with ethanol, and dried under vacuum at 60℃ for 6 h. As-prepared N-type thermoelectric composite films are denoted as 1D CP-SL/PEI-CNT_x, where x indicates the CNT weight fraction (wt.%).

Type	CNT (g)	CP-SL(g)	PEI(g)
1D CP-SL/PEI-CNT_{30}	0.0085	0.020	1.8
1D CP-SL/PEI-CNT_{20}	0.010	0.041	1.8
1D CP-SL/PEI-CNT_{10}	0.010	0.087	1.8
1D CP-SL/PEI-CNT_{5}	0.010	0.099	1.8
1D CP-SL/PEI-CNT_{1}	0.004	0.330	1.8

Fabrication of compressed 1D CP-SL/CNT and 1D CP-SL/PEI-CNT composite films

All of p/n type of CP-SL/SWCNT composites strips were cut into rectangular strips of 20 mm in length and 4 mm in width. The composite strips were placed between two pieces of polyethylene terephthalate (PET) films, then placed on a tablet press. A pressure of 30 MPa was applied and held for a certain time (0.17~2 h). The compressed p/n type of composites strips were peeled off from the PET films.

Fabrication of flexible thermoelectric generator

Flexible thermoelectric generators (TEGs) were fabricated by compressed CP-SL/CNT film strips and compressed CP-SL/SWCNT film strips for p-type and n-type legs, respectively. The films were fabricated by a pressure of 30 MPa for 30 min as previously described. The films were cut into rectangular of 30 mm in length and 4.3 mm in width. The thickness of the strips is 10 μm. These p-type and n-type legs were arranged alternately a series of six p-n juntions. Then, the composite strips were connected in series with silver paste and copper foil. The pieces of copper foil were attached to both ends of the device with silver paste to ensure contact with the electrodes and the thermoelectric legs to detect the performance using a probe station. All the p-type and n-type film strips were arranged on an insulated polyimide film. TEG thermoelectric performances were test in cold temperature and high temperature at a gradient of 180 K and 100 K, respectively. The cold temperature gradient across the TEG were controlled by liquid nitrogen, the hot sides were in the air which held constant at 298 K. Temperature gradients were established by adjusting the immerse height into the liquid nitrogen. The high temperature gradient was controlled using a constant temperature heating plate. The hot sides of the high temperature were obtained by a heating plate, and the cool sides were placed in air at 298 K. The equation of the temperature gradient (ΔT) is $\Delta T = T_{hot} - T_{cold}$. The temperature at both ends of the strips was measured using a thermocouple. The effective device area is 1548 mm^2 containing all the p and

n strip area. The area used for calculating the output power density is 5.16×10^{-7} m^2 (the total cross-sectional area of all p and n strips (leg width $\times$ leg thickness for each of the six p-n pairs).

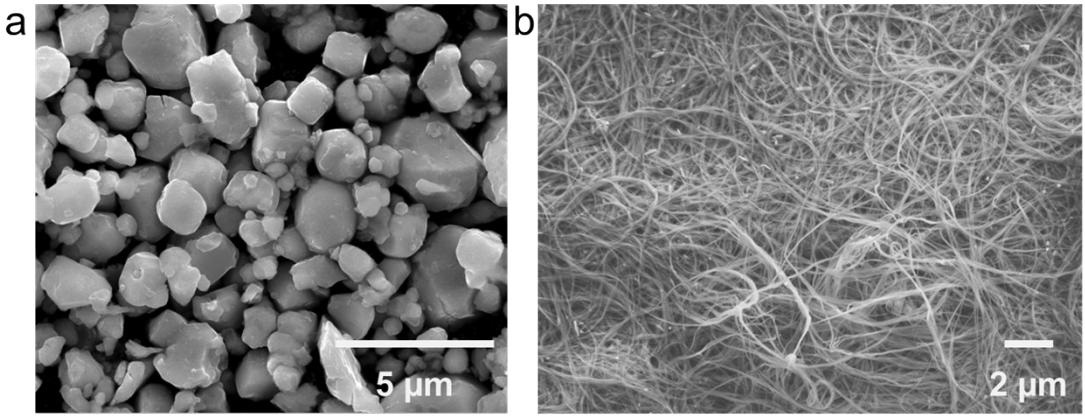

Figure S1 SEM of Cu_2O (a) and 1D CP-SL (b).

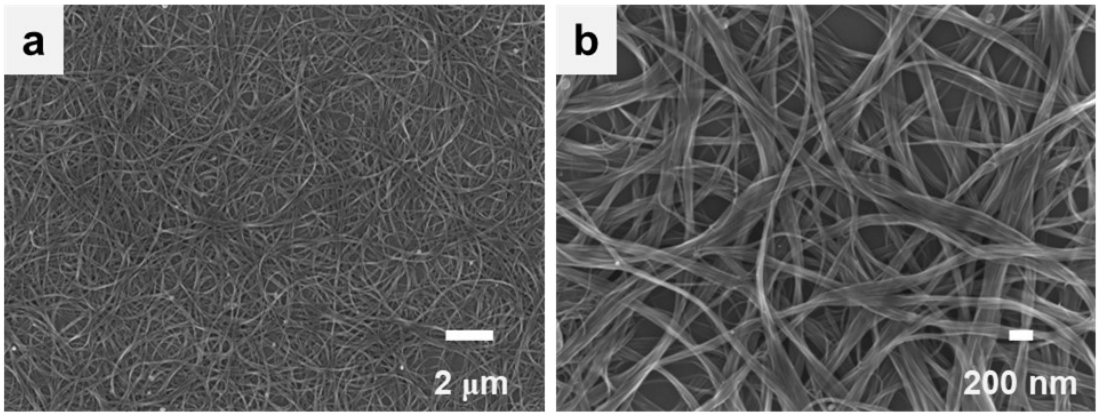

Figure S2 The SEM of the dispersion CNTs.

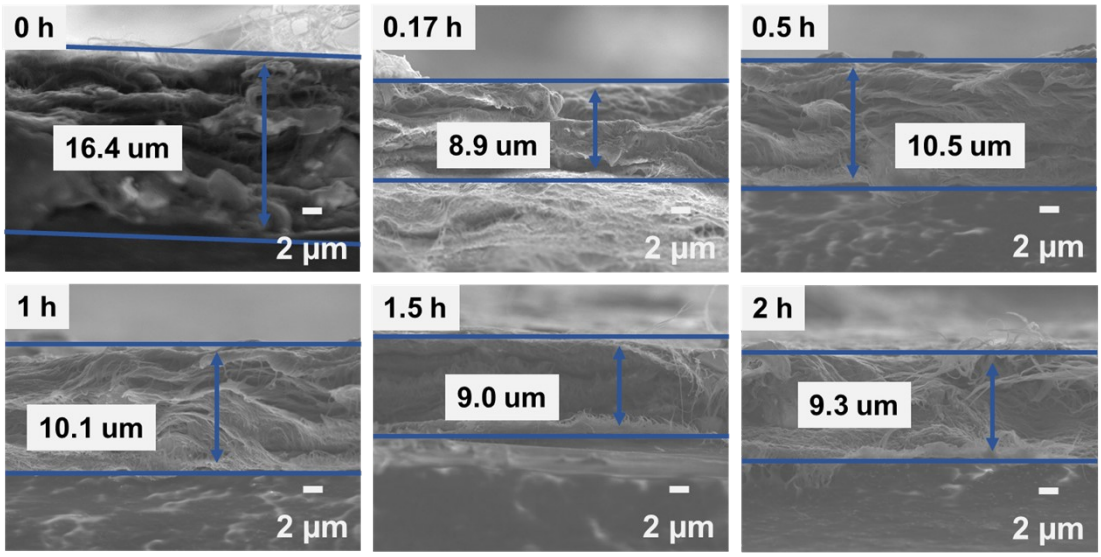

Figure S3 The SEM of the cross-section for 1D CP-SL/CNT_{50} film under different compressing time.

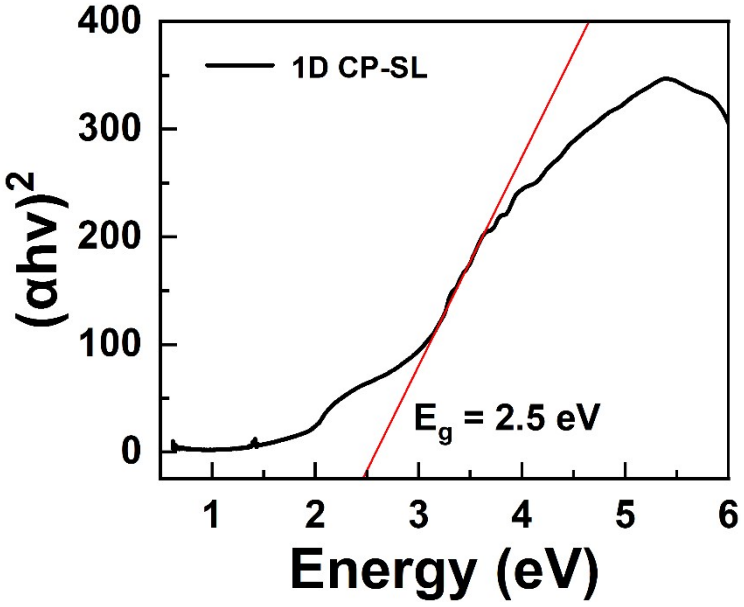

Figure S4 The optical band gap of 1D CP-SL.

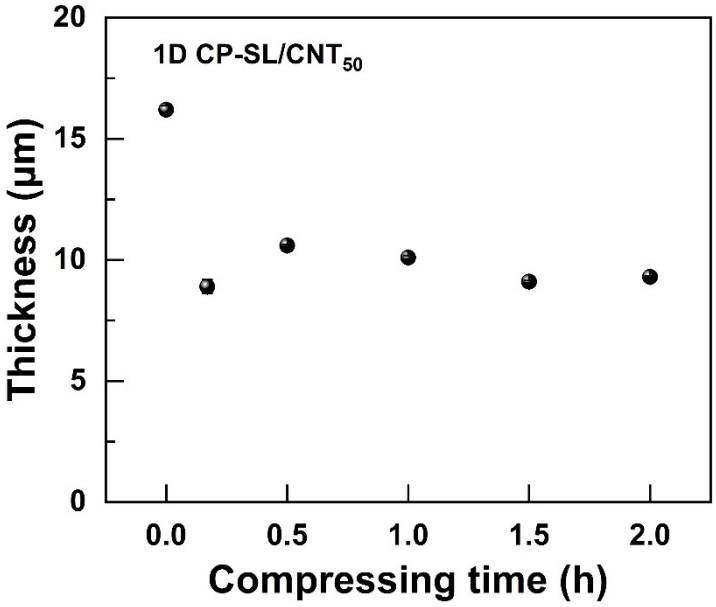

Figure S5 The statistical plots cross-section thickness of 1D CP-SL/CNT_{50} under different compressing time.

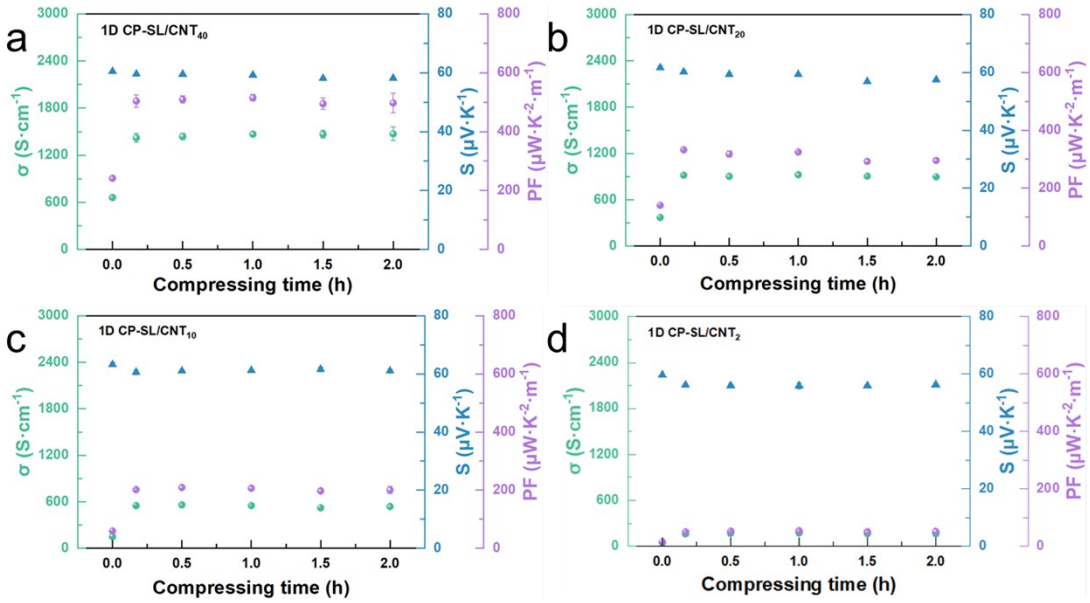

Figure S6 The electrical conductivity and Seebeck coefficient with compressing time of 1D CP-SL/CNT_{40} (a), 1D CP-SL/CNT_{20}(b), 1D CP-SL/CNT_{10} (c), 1D CP-SL/CNT_2 (d).

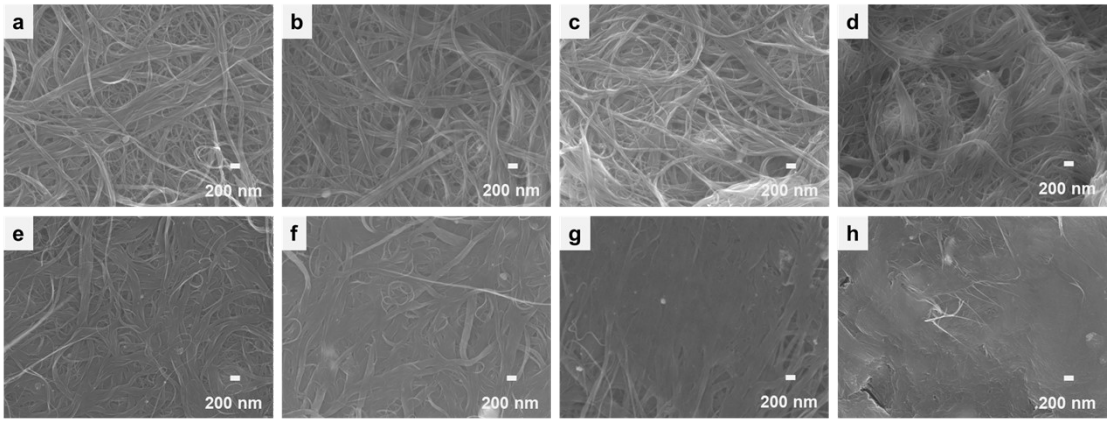

Figure S7 The SEM of unpressed 1D CP-SL/CNT_{40} (a), unpressed 1D CP-SL/CNT_{20} (b), unpressed 1D CP-SL/CNT_{10} (c), unpressed 1D CP-SL/CNT_2 (d), the pressed 30min 1D CP-SL/CNT_{40} (e), the pressed 30min 1D CP-SL/CNT_{20} (f), the pressed 30min 1D CP-SL/CNT_{10} (g), the pressed 30min 1D CP-SL/CNT_2 (h).

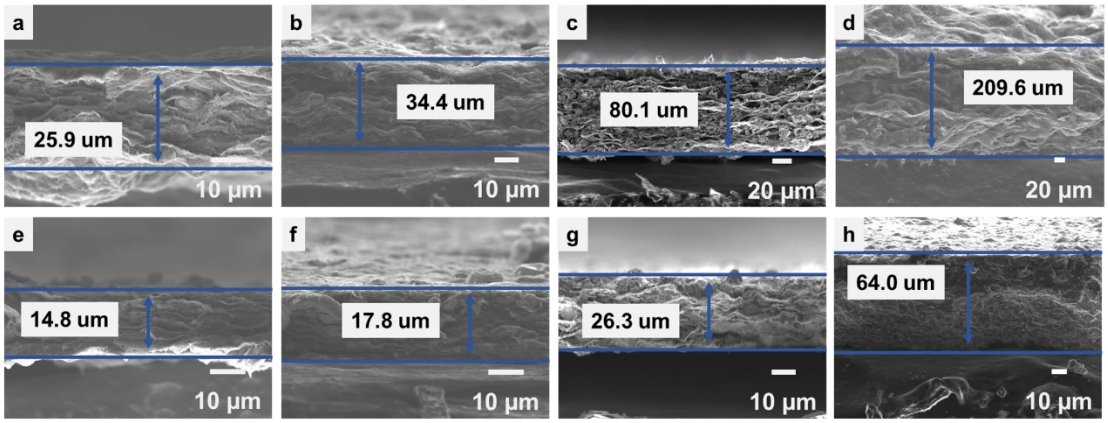

Figure S8 The SEM of the cross-section for unpressed 1D CP-SL/CNT_{40} (a), unpressed 1D CP-SL/CNT_{20} (b), unpressed 1D CP-SL/CNT_{10} (c), unpressed 1D CP-SL/CNT_2 (d), pressed 30min 1D CP-SL/CNT_{40} (e), pressed 30min 1D CP-SL/CNT_{20} (f), pressed 30min 1D CP-SL/CNT_{10} (g) and pressed 30min 1D CP-SL/CNT_2 (h).

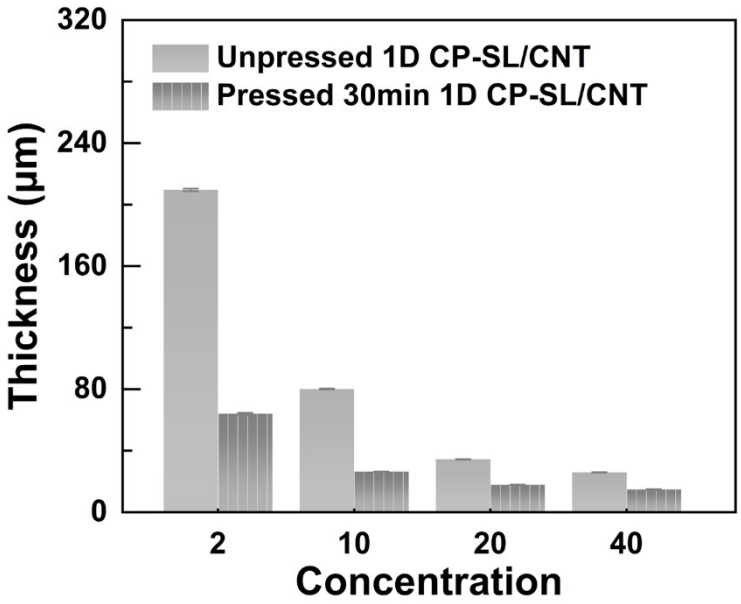

Figure S9 The statistical plots cross-section thickness of 1D CP-SL/CNT under different compressing time.

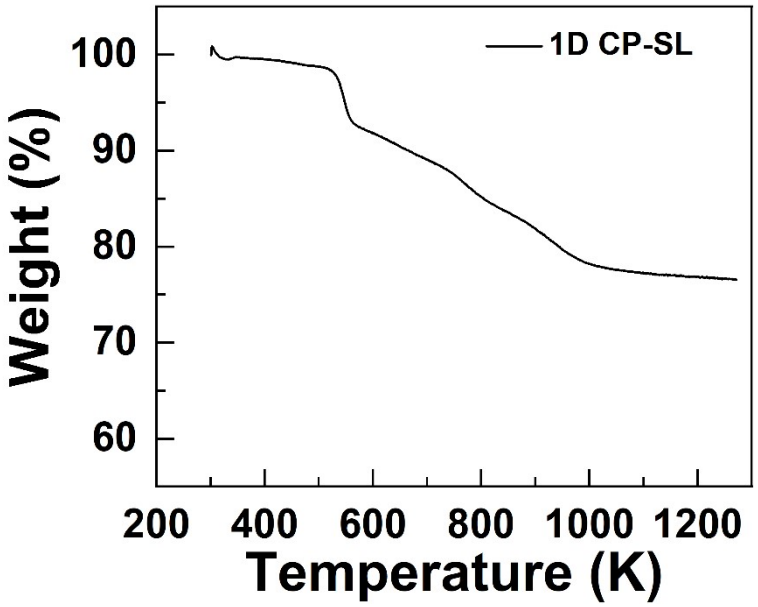

Figure S10 TGA of 1D CP-SL.

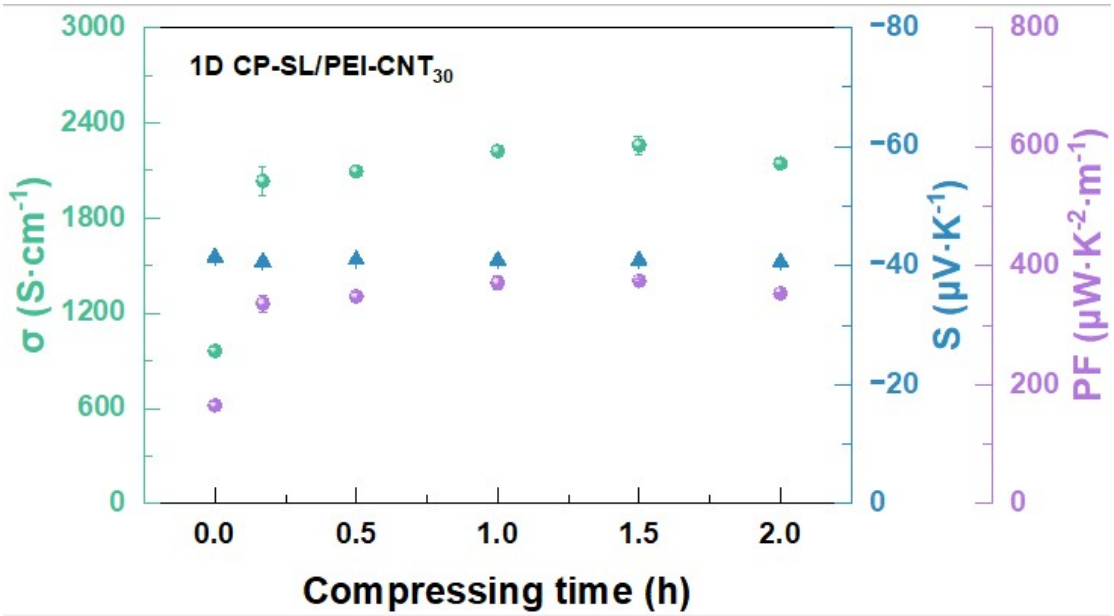

Figure S11 The electrical conductivity, Seebeck coefficient and PF of CP-SL/PEI-CNT_{30} with different compressing time.

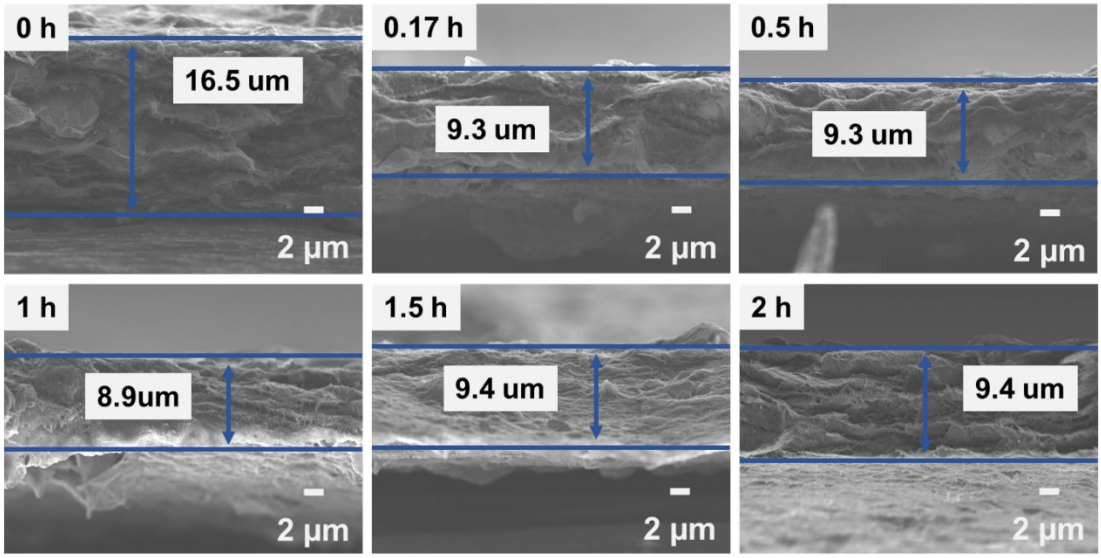

Figure S12 The SEM of the cross-section for 1D CP-SL/PEI-CNT_{30} film under different compressing time.

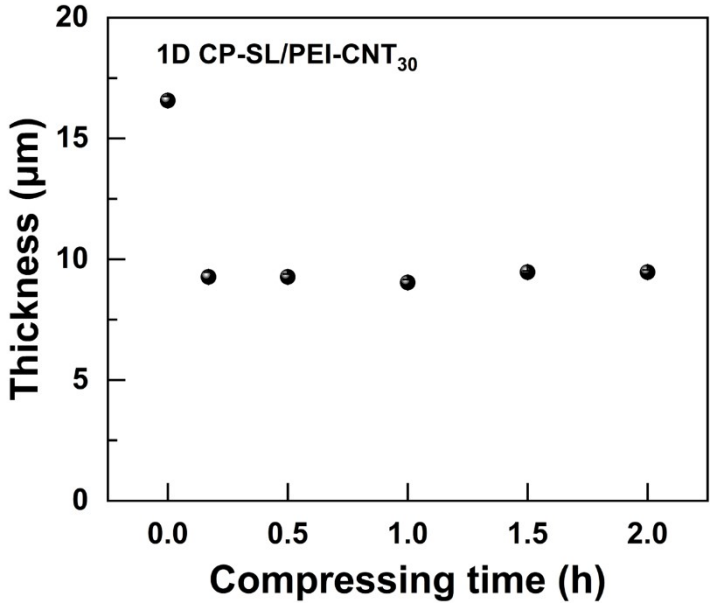

Figure S13 The statistical plots cross-section thickness of 1D CP-SL/PEI-CNT_{30} under different compressing time.

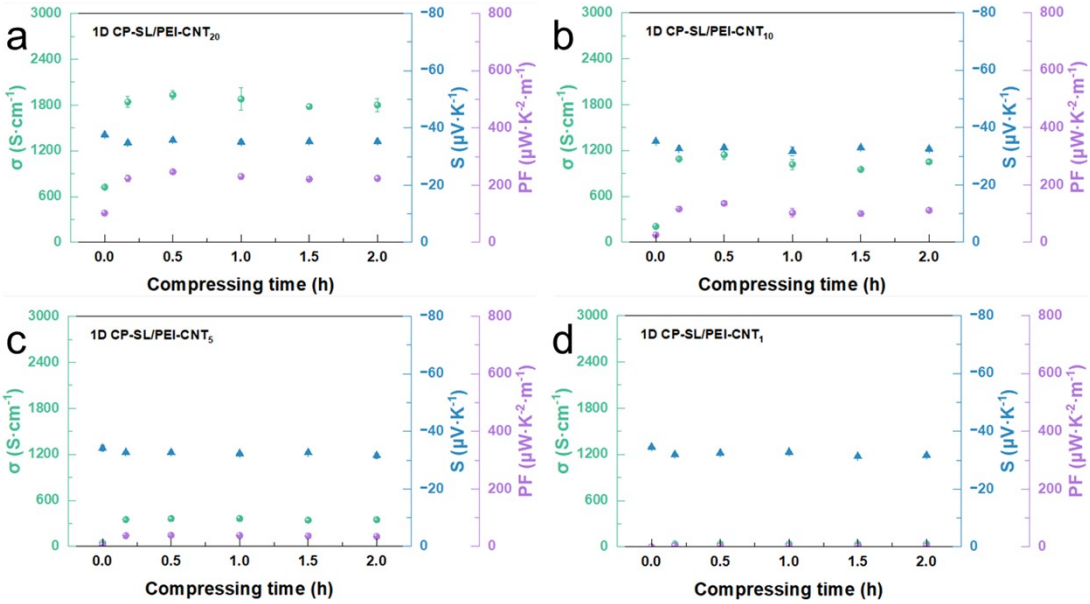

Figure S14 The electrical conductivity and Seebeck coefficient with different compressing time for 1D CP-SL/PEI-CNT_{20} (a), 1D CP-SL/PEI-CNT_{10} (b), 1D CP-SL/PEI-CNT_5 (c), 1D CP-SL/PEI-CNT_1 (d).

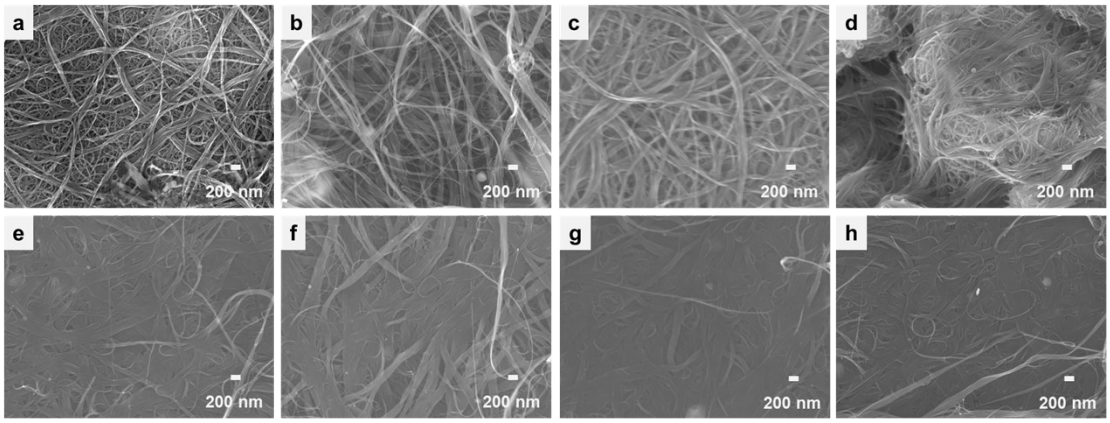

Figure S15 The SEM of unpressed 1D CP-SL/PEI-CNT_{20} (a), unpressed 1D CP-SL/PEI-CNT_{10} (b), unpressed 1D CP-SL/PEI-CNT_5 (c), unpressed 1D CP-SL/PEI-CNT_1 (d), the pressed 30min 1D CP-SL/PEI-CNT_{20} (e), the pressed 30min 1D CP-SL/PEI-CNT_{10} (f), the pressed 30min 1D CP-SL/PEI-CNT_5 (g), the pressed 30min 1D CP-SL/PEI-CNT_1 (h).

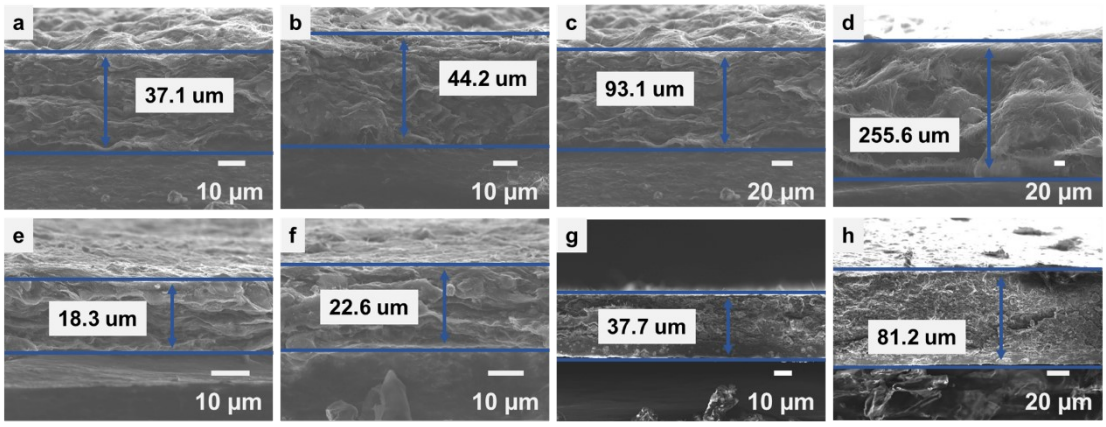

Figure S16 The SEM of the cross-section for unpressed 1D CP-SL/PEI-CNT_{20} (a), unpressed 1D CP-SL/PEI-CNT_{10} (b), unpressed 1D CP-SL/PEI-CNT_5 (c), unpressed 1D CP-SL/PEI-CNT_1 (d), pressed 30min 1D CP-SL/PEI-CNT_{20} (e), pressed 30min 1D CP-SL/PEI-CNT_{10} (f), pressed 30min 1D CP-SL/PEI-CNT_5 (g) and pressed 30min 1D CP-SL/PEI-CNT_1 (h).

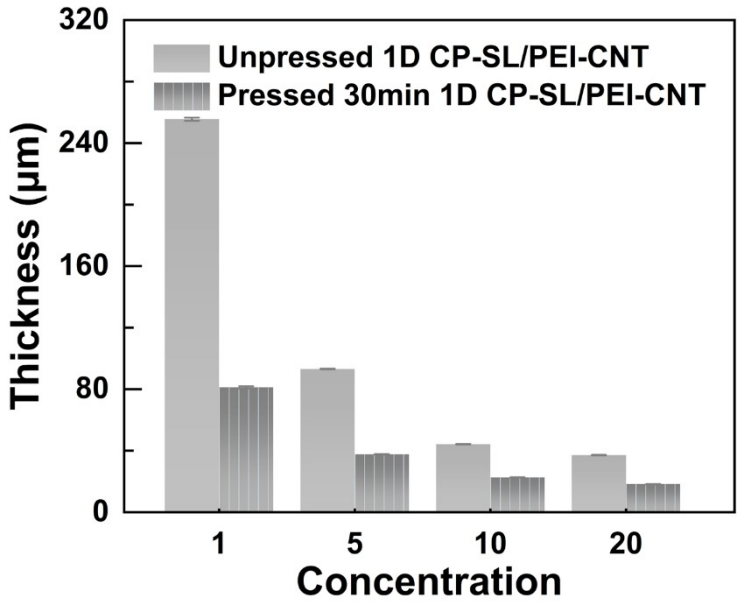

Figure S17 The statistical plots cross-section thickness of 1D CP-SL/CNT under different compressing time.

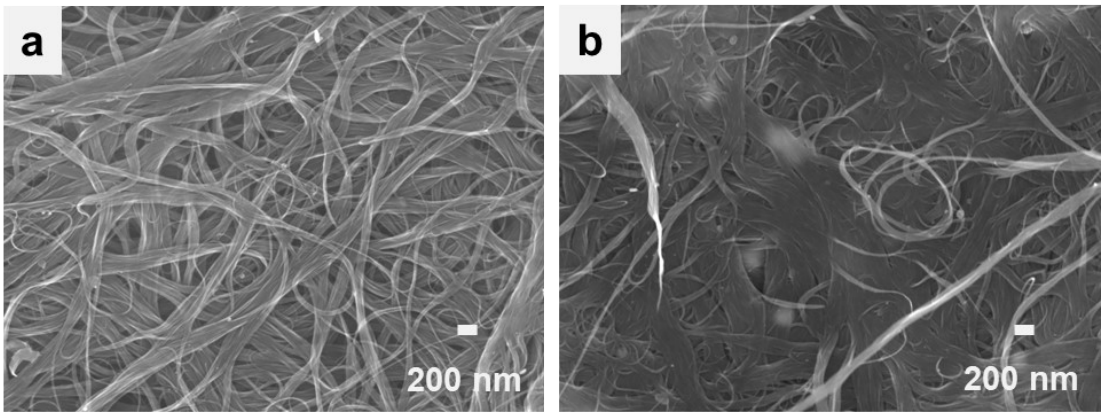

Figure S18 The SEM of unpressed 1D CP-SL/PEI-CNT_{30} (a) and pressed 30 min CP-SL/PEI-CNT_{30} (b)

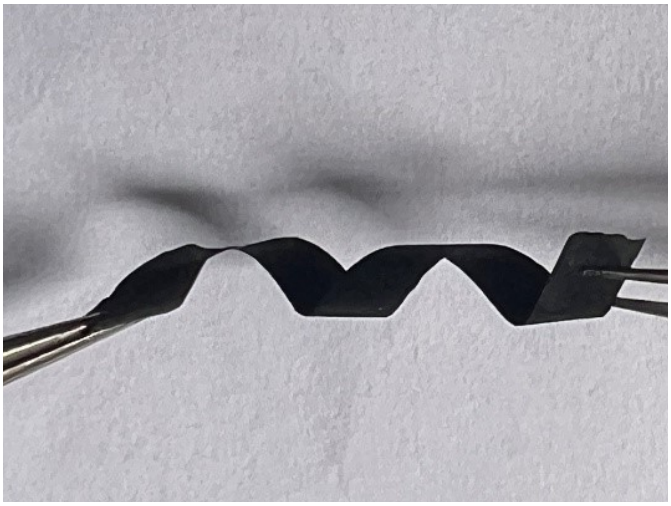

Figure S19 The optical photograph of the flexibility of 1D CP-SL/PEI-CNT_{30}.

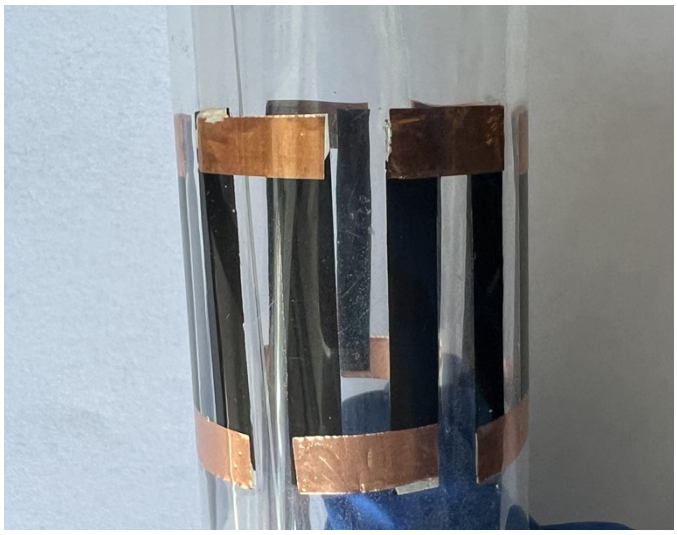

Figure S20 The optical photograph of the flexibility of the flexible TEG.

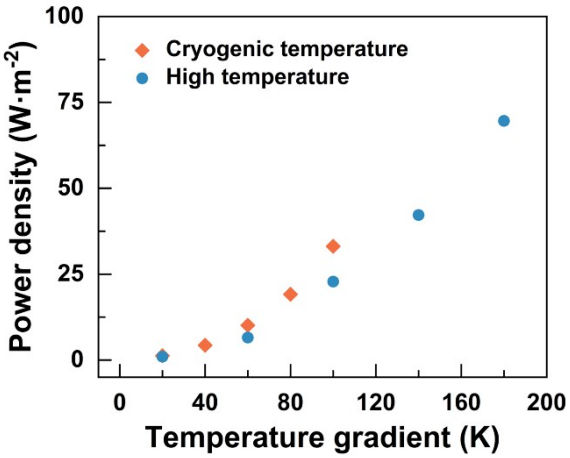

Figure S21 The power density of the TEG device under different temperature gradients.

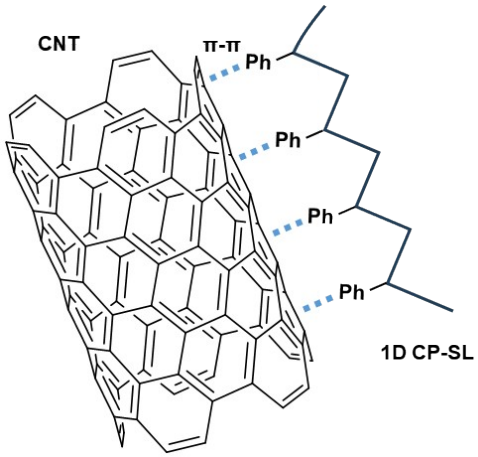

Figure S22 Schematic illustration of π-π stacking between MOF and CNTs.

Table S1: Comparison of reported PF values and σ of various MOF/CNTs TE materials.

No.	Materials	Thk. (μm)	σ ($S \cdot cm^{-1}$)	PF ($\mu W \cdot m^{-1} \cdot K^{-2}$)
1[4]	MIL-53(Al)/CNT, CNT30%	25	118.5	4.4
2[5]	$Ni_3(HITP)_2/CNT_{30}$, CNT30%	1500	150	24.86
3[6]	Fc-P_1/SWCNT, CNT90%	2	1050.8	367.4
4[7]	CP-SL/CNT, CNT30%	3000	226.3	19.03
5[8]	(PEDOT:PSS)/CNTs/M-UIO-66, CNT45wt%	/	486.3	27.9
6[9]	SWCNT@THT, CNT4wt%	30	590	98.1
7[10]	Cu-MOF/CNT	/	729.3	221.8
8[11]	ZIF-67@CNT	/	825.7	255.6
9[3]	CP-SL/CNTs, CNT30wt%	14.3	1130	140
10[12]	MOF/CNT_{10}	10	1167.1	395.2
11[13]	$CNT/ZrBTBD_{10}$	5	1172	465.7
This work	1D CP-SL/CNT_{50}, CNT50%	10.5	1830	630

Table S2: Comparison of reported TEG devices properties of MOF/CNTs.

No.	Device leg	Open-circuit voltage	Output power of TEG
1[4]	14	11.20 mV (30 K)	0.17 μW
2[5]	8	3.27 mV (60 K)	0.07 μW
3[6]	10	None (72 K)	1.18 μW
4[7]	8	6.68 mV (39.7 K)	0.53 μW
5[9]	4	10.02 μV(60 K)	1.59 μW
6[3]	12	53.00 mV (180 K)	19.00 μW
This work	12	Low Temp.:78 mV（180 K） High Temp.:54 mV（100 K）	Low Temp.:35.90 μW（180 K） High Temp.:17.10 μW（100 K）

References:

1. K.-H. Low, V. A. L. Roy, S. S.-Y. Chui, S. L.-F. Chan and C.-M. Che, *Chem. Commun.*, 2010, **46**, 7328-7330.
2. Y. Li, J. Shu, Q. Huang, K. Chiranjeevulu, P. N. Kumar, G.-E. Wang, W.-H. Deng, D. Tang and G. Xu, *Chem. Commun.*, 2019, **55**, 10444-10447.
3. Q. Guo, J. Wang, T. Zhuang, Y. Liu, F. Yin and H. Wang, *Journal of Materials Chemistry A*, 2025, **13**, 37997-38008.
4. M.-H. Lin, C.-H. Hsu, D.-Y. Kang and C.-L. Liu, *Chem. Eng. J.*, 2024, **485**, 149732.
5. X. Qi, Y. Wang, K. Li, J. Wang, H.-L. Zhang, C. Yu and H. Wang, *Journal of Materials Chemistry A*, 2021, **9**, 310-319.
6. Z. Sun, Z. Ma, X. Zhou, Y. Wang, J. Zhang and W.-Y. Wong, *Journal of Materials Chemistry A*, 2024, **12**, 22061-22069.
7. K. Li, L. Xu, Z. Li, Y. Wang, J. Wang, X. Qi, Q. Li and H. Wang, *Nano Energy*, 2021, **84**, 105902.
8. Y. Fan, Z. Liu and G. Chen, *Composites Communications*, 2022, **29**, 100997.
9. Z. Chen, Y. Cui, L. Liang, H. Wang, W. Xu, Q. Zhang and G. Chen, *Materials Today Nano*, 2022, **20**, 100276.
10. G. Tian, J. Zhang, Z. Li, L. Guo, P. Fu, C. Tang, C. Tsui, Y. Zhang and F. Du, *J. Power Sources*, 2025, **630**, 236121.
11. Y. Xue, Z. Zhang, Y. Zhang, X. Wang, L. Li, H. Wang and G. Chen, *Carbon*, 2020, **157**, 324-329.
12. C.-Y. Lin, J.-W. Chang, M.-H. Lin, K.-C. Wu, S.-H. Hong, J.-M. Lin, C.-W. Kung and C.-L. Liu, *Chem. Eng. J.*, 2025, **521**, 166861.
13. C.-Y. Lin, K.-C. Wu, C.-W. Hsu, S.-H. Hong, C.-L. Chuang, T.-J. Hsu, J.-M. Lin, C.-W. Kung and C.-L. Liu, *ACS Nano*, 2026, **20**, 12425-12439.